

Sensorless-Voltage Control for a grid Tied Inverter Using Disturbance Observer with Net Metering

¹P. Saravana Kumar*, ²Dr.S. Sutha Padmanabhan,
 Research scholar/EEE, Associate Professor/EEE,
 University College of engineering, Dindigul.

Abstract

A grid tied inverter mainly required voltage and current measurement to reactive power and active power or else inverter output current. Voltage sensors are reliable information on the phase angle using these additional components increase the cost of production and system complexity. In this paper, sensorless voltage control for a grid tied inverter using disturbance observer with net meter is presented. The grid voltage is estimated by disturbance observer in the stationary frame reference using the reference signal and current measurement. The disturbance observers estimate the grid voltage with reasonable accuracy with Presence variable such as the unbalanced condition and harmonics distortion. The result waveforms shows that a phase leg depending on the estimation bandwidth.to outcome this limitation, a phase lead compensation is newly introduced.by using these new concept phase angle of a grid voltage can be completely restored. If the phase angle of grid is initially unknown. New technology based Proposed Sensorless voltage control experiments using 2KVA prototype inverter.

Keywords: Disturbance observer (DOB), estimation of grid voltage and phase angle, Distributed generation (DG), Grid tied inverter, Sensorless voltage control.

1. INTRODUCTION

Solar based grid tied inverter most commonly rated by the continuous output power (AC) capability the wattage of the inverter output continuously. A continuous load is defined as a load where the maximum is expected to continuous for 3 hours or more than that. All circuit integrated with grid tied PV systems, on the both AC and DC sides of the inverter are considered continuous. This continuous power getting the PV arrays maximum power value. Grid tied inverter will limit the output power. If design the array that supplies more power than the inverters maximum, the inverter not able to process all power. Instead, the inverter will waste of any excess power as a heat. In this case will all the electronics, getting unnecessary heat reduce the inverter life. PV arrays produce less than their STC power rating mostly to conditions that differ from STC power like a higher cell temperature, lower irradiance and module soiling when predicable system losses are taken into the account. PV system we can expect their array to operate at around 80% of the STC rating. Since these losses are consistently, present the size of the PV array can be designed to exceed the inverter power rating. Many inverters. Manufactures specify that a PV arrays STC rathing should be not more than 125% of the inverters continuous output power rating. As the sizing ration. If an inverter has a continues output power rating 5000w, the maximum array size that be connected using the size ratio of 1.25 would be 6250W (5000w * 1.25).

II.DESIGN OF GRID VOLTAGE WITH DISTURBANCE OBSERVER

The main objective of the control design is to steer the state yto its desired reference value in thepresence of external disturbance *d* such as the harmonics and imbalance, and at the same time, to obtain the phase angle information by design the grid voltage with DOB.

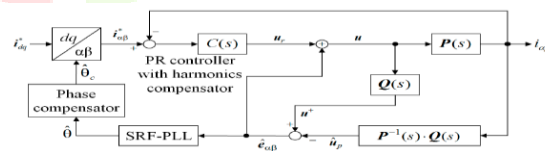


Figure 1: overall block diagram of proposed Sensorless-voltage

$$y = Ay + Bu - Bd \text{ ----- (1)}$$

From above, the disturbed control input can be calculated as follows:

$$u - d = B^{-1}(y - Ay) \text{ ----- (2)}$$

With $u = v_{\alpha\beta}$ in above Equation the disturbed control input $u - d$ can be expressed as

$$u - d = P^{-1}(s)y \text{ -----(3)}$$

Theoretically, $u - d$ can be calculated from the *y* output if the system inverse model $P^{-1}(s)$ is realizable. However, because $P^{-1}(s)$ is not proper in general, a stable filter $Q(s)$ such as a lowpass filter (LPF) is required in the implementation of the DOB in order that $P^{-1}(s)Q(s)$ is proper. Selecting Q as the first-order LPF, the disturbed system input $u - d$ is now modified to the filtered value as follows:

$$u - d = P^{-1}(s)Q(s)y \text{ ----- (4)}$$

Figure shows various grid voltages used for test purpose, which are generated by three-phase programmable AC power source figure 5a represents the ideal grid voltage in which the frequency.is 60 Hz and the line-to-line voltage is 220 V in root-mean-square (RMS). Figure 5b shows three-phase unbalanced grid voltages with 20% magnitude reduction in *c*-phase. Figure 5c shows the harmonic distorted grid voltages including 5% of the fifth- and seventh-order harmonics, respectively.

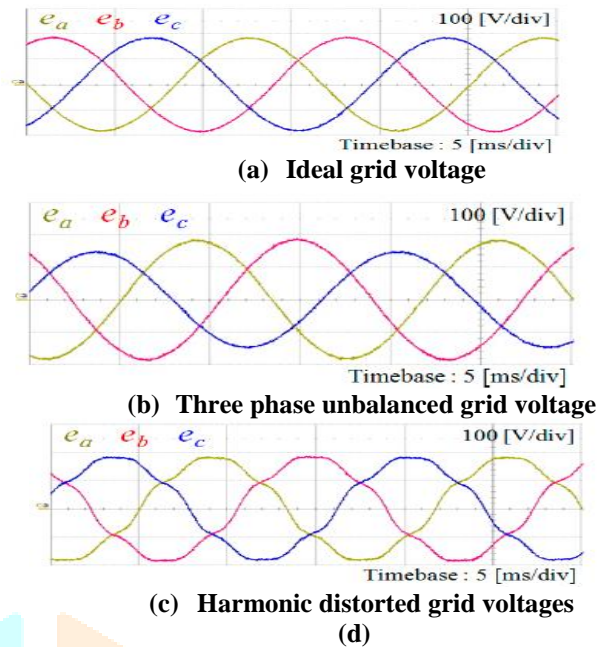


Figure 2: Existing system grid voltage and proposed grid voltage

III.MPPT FUNCTION

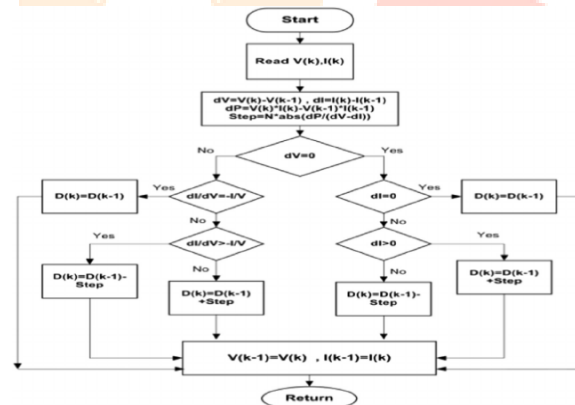


Figure 3: Block diagram of MPPT Function

The block diagram is an explanation of the perturb and observe (P and O) method, a very common and easy way to implement an MPPT technique. The PV array voltage is compared to a constant reference voltage, which corresponds, once the algorithm has reached the convergence, to the PV array voltage at the maximum power point, under specific atmospheric and temperature conditions. The error signal is used as the input of a PI regulator which generates a command (phase-shift angle) used to drive the power devices of the DC-DC converter.

IV. PROPOSED SYSTEM OF SENSORLESS-VOLTAGE CONTROL OF A GRID CONNECTED INVERTER

The proposed Sensorless-voltage control system which Design the phase angle of the grid voltage is explained using above Figure. The q-axis and d-axis current i_{dq} * value are first transformed into the stationary values using the design phase angle. The PR current controller is designed for a grid tied inverter in the stationary Design frame. At the same time, the grid voltages are Design through the DOB by comparing the reference voltages with the current information processed with the design system inverse model. The Design of grid voltage $e_{\alpha\beta}$ in Equation

$$\hat{d} = u^+ - \hat{u}_p \text{ ----- (5)}$$

Output of the DOB, is used to compose the design reference voltage signal u as well as to generate the phase angle $\hat{\theta}$ through the synchronous reference frame PLL (SRF-PLL).

From the LPF $Q(s)$ in $\dot{q} = A_q q + B_q y$ ----- (6)

The transfer function of the first element can be obtained as follows:

$$Q_{11}(s) = \frac{a0/T}{s+a0/T} \text{ ----- (7)}$$

From above equation, the phase delay at the grid frequency introduced by the LPF can be simply calculated as follows:

$$\theta_{delay} = \angle Q_{11}(j\omega_g) = -\tan^{-1}(\tau\omega_g / a0) \text{ - (8)}$$

Where ω_g denotes the grid angular frequency and θ_{Delay} denotes the phase delay due to the LPF in DOB.

$$\hat{\theta}_c = \hat{\theta} + \theta_{Delay} \text{----- (9)}$$

V. IMPLEMENTED CONTROL ALGORITHM

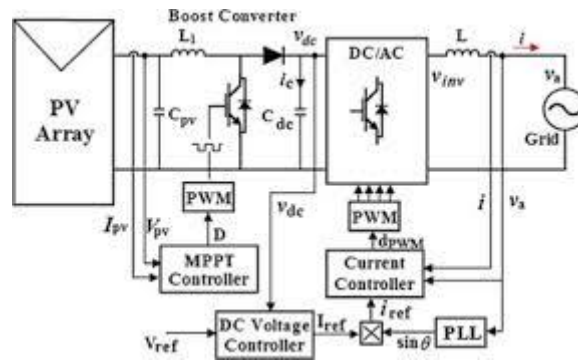


Figure 4: Implemented control algorithm grid tied system

VI. DESIGN EXAMPLE:

The design is based on the core geometry method. The transformer specifications are shown in Table 1:

Table1: HF transformer specifications

Specifications	symbol	value
Nominal input voltage	Vin	300V
Maximum input voltage	Vinmax	400V
Minimum input voltage	Vinmin	200V
Input current	Iin	27A
Nominal output voltage	Vout	450V
Output current	Iout	22.2A
Switching frequency	f	35KHZ
Efficiency	η	99%
Regulation	α	0.15
Max operating flux density	Bm	0.15T
Window utilization	Ku	0.3
Duty cycle	Dmax	0.5
Maximum temperature rise	Tr	70°C

DC-AC Converter

The value of Lf is designed in order to limit the current ripple to about 10 % of the nominal current value according to:

$$L_f = \frac{(V_{BUS} - V_{grid_pk}) \cdot D}{2 \cdot \Delta i \cdot f_{sw}} = \frac{(450 - 324) \cdot 0.72}{2 \cdot 1.3 \cdot 17000} = 2.05mH \text{---(10)}$$

The filter capacitor value is designed to limit the exchange of reactive power below 5 % of nominal active power:

$$P_{reactive} = \frac{V^2_{grid}}{0.05 P_n} \leq 0.05 P_n$$

$$X_c \geq \frac{V^2_{grid}}{0.05 P_n} = 352.6\Omega$$

$$C \geq \frac{1}{\omega X_c} = 9\mu f$$

To avoid resonance problems for the filter, due to low and high order harmonics, its resonant frequency, given by

$$f_{res} = \frac{1}{2\pi} \sqrt{\frac{L_g + L_f}{L_f L_g C_f}}$$

Should be in a range between ten times the line frequency and one half of the switching frequency:

$$10 * f_{grid} \leq f_{res} \leq 0.5 f_{sw}$$

$$500HZ \leq f_{res} \leq 8.5KHZ$$

The power losses in each IGBT may be calculated considering conduction losses, switching losses and diode losses. Conduction and switching losses in IGBTs may be evaluated according to the following equations:

$$P_{cond} = V_{CE} * I_{pk} \left(\frac{1}{2\pi} + \frac{1}{8} ma \cos \phi \right) + R_{CE} * I^2_{pk} * \left(\frac{1}{8} + \frac{ma}{3\pi} \cos \phi \right) = 9.6w \text{----- (11)}$$

Where

$$V_{CE} = 1.8V$$

$$ma = \frac{V_{grid_pk}}{V_{bus}} = \frac{325}{450} = 0.72$$

$$\cos \phi = 1$$

$$P_{diode_DC} = V_F * I_{pk} * \left(\frac{1}{8} - \frac{ma}{3\pi} \cos \phi \right) = 1.3w$$

$$P_{diode_RR} = \frac{1}{8} I_{rr} t_{rr} V_{pk} f_{sw} = 0.45w$$

$$V_{pk} = 450V, I_{rr} = 5.4A, t_{rr} = 88ns$$

$$P_{tot} = 4(P_{diode-DC} + P_{diode-RR} + P_{sw-on} + P_{sw-off} + P_{cond}) \dots \dots \dots (12)$$

Result in 98% theoretical efficiency for the inverter stage. A simple modification of the control strategy, together with a different choice of power devices, may improve the efficiency and performance of the DC-AC stage. The modified circuit is shown in below figure.

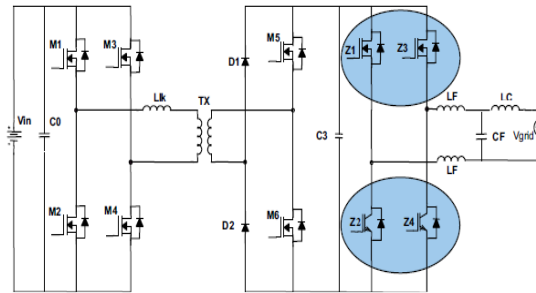


Figure 5: Conversion system with modified DC-AC inverter

Every algorithm for grid-connected inverter operation is based on the estimation or direct measurement of grid-voltage frequency and phase angle. Both parameters are fundamental for correct operation and special care must be taken in their detection to avoid the influence of any external noise. The detection method used in this implementation for a single-phase inverter is based on a synchronous reference frame PLL. While in three-phase inverters the use of DQ based PLL is quite common, for single-phase inverters, the necessity of a virtual bi-phase system arises. In fact, to create a rotating DQ reference, starting from a stationary reference frame, at least two independent phases are required. This problem is overcome with the creation of a virtual voltage, $V\beta$, phase-shifted with respect to the real power grid voltage $V\alpha$, of 90° . This task may be easily accomplished with firmware. If the two voltage components $V\alpha$ and $V\beta$ are available, the transformation from the stationary reference frame to the DQ rotating frame is given by:

$$\begin{bmatrix} V_d \\ V_q \end{bmatrix} = \begin{bmatrix} \cos \theta & \sin \theta \\ -\sin \theta & \cos \theta \end{bmatrix} \begin{bmatrix} V_\beta \\ V_\alpha \end{bmatrix} \dots \dots \dots (13)$$

Where θ is the angle between the DQ reference frame and the stationary reference frame. Figure 3 shows the reverse transformation is given by,

$$\begin{bmatrix} V_\beta \\ V_\alpha \end{bmatrix} = \begin{bmatrix} \cos \theta & -\sin \theta \\ \sin \theta & \cos \theta \end{bmatrix} \begin{bmatrix} V_d \\ V_q \end{bmatrix} \dots \dots \dots (14)$$

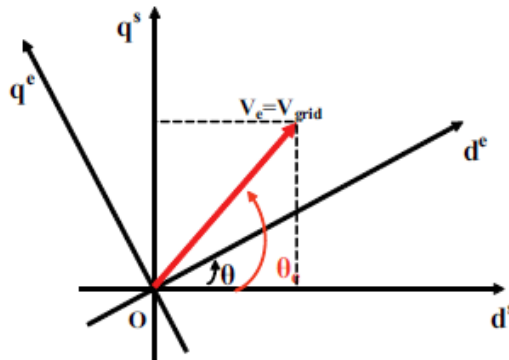


Figure 6: stationary reference frame and rotating Reference frame

$$\begin{bmatrix} V_\beta \\ V_\alpha \end{bmatrix} = \begin{bmatrix} V_m \cos \theta_\theta \\ V_m \sin \theta_\theta \end{bmatrix} \dots \dots \dots (15)$$

Then the two components on the DQ reference frame are:

$$V_d = V_m \cos \theta_\theta \cos \theta + V_m \sin \theta_\theta \sin \theta = V_m \cos(\theta - \theta_\theta) \dots \dots \dots (16)$$

$$V_q = -V_m \cos \theta_\theta \sin \theta + V_m \sin \theta_\theta \cos \theta = V_m \sin(\theta - \theta_\theta) \dots \dots \dots (17)$$

Therefore, if $\theta = \theta_\theta$ the two components are reduced:

$$V_d = V_m \dots \dots \dots (18)$$

$$V_q = 0 \dots \dots \dots (19)$$

In order to detect the grid-voltage angle, used to perform the transformation, a PLL structure may be used. In Figure 4, the block diagram of the PLL implemented in this application is shown.

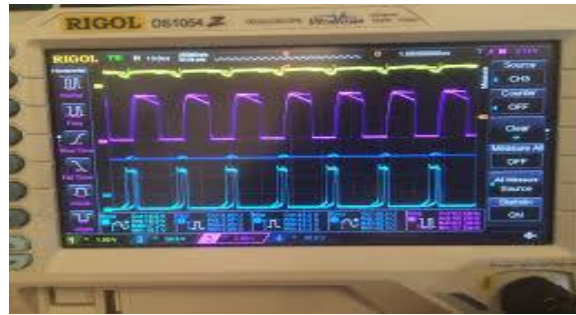


Figure10: DC-DC Switching frequency and AC-DC switching frequency.

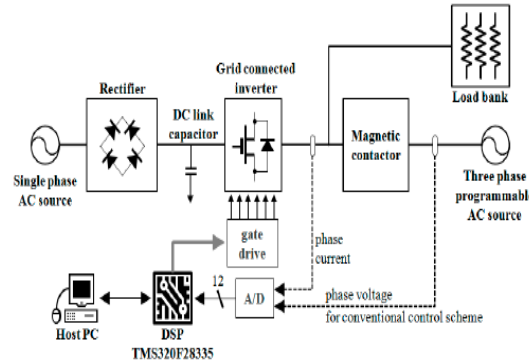


Figure 11: configuration of overall system

TEST REPORT OF UNITY GRID:

UNITS	Utility power one(NO GTI)*		With GTI that displaces 50% of utility real power(KW)***	
	@Utility meter (initial power factor)	@GTI output	@Utility meter (initial Power Factor)	@GTI output
Before				
PF	0.912	N/A	0.743	1
KW	3	N/A	1.5	1.5
KVRS	1.2	N/A	1.5	0
KVA	3.8	N/A	1.2	1.5
AFTER				
PF	3.8	N/A	1.9	1
PF	0.955	N/A	0.85	1
KW	3	N/A	1.5	1.5
KVRS	1	N/A	1	0
KVA	3.6	N/A	1.8	1.5

3. Proposed work Result.

To verify the feasibility of the proposed scheme, Figure 11 illustrates the comparative simulation results for the inverter output currents under the ideal grid condition between the conventional scheme with voltage measurements and the proposed voltage Sensorless control scheme. It is obvious from these figures that the control performance of the proposed scheme is comparable to the case with voltage measurement. Comparison of inverter output currents under the ideal grid condition.

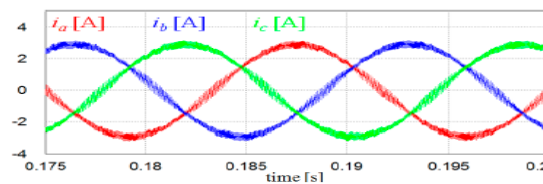


Figure 12 (a) Inverter output current with voltage measurements

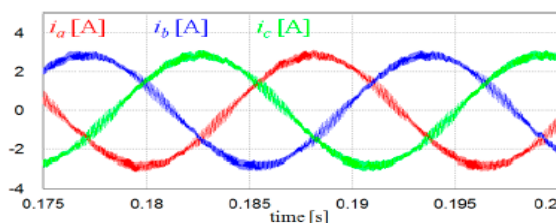


Figure 12(b) Inverter output current with the proposed voltage-Sensorless control

VIII. RESULTS AND FUTURE WORK

The hardware setup, i.e. the board is finished and tested. A photo of the complete board is shown in Fig. 8. In the background the power stage with the MOSFETs, inductors and DC-link capacitors is visible. More in the foreground the DSP-controller and the analog circuitry can be seen. The basic software framework is coded and tested, too. At the moment we are at the stage of implementing the control sub modules and the GUI. We will continue the development and will demonstrate the setup in different configurations at MNRE Specification of Electricity board.

IX. CONCLUSION

To obtain the information of grid voltage without using the voltage sensors, the proposed method of DOB based technique to estimate the grid voltage from the reference signal and current measurements. By using the proposed DOB based with a phase lead compensation, the phase angle of grid voltage can be completely restored even the phase angle of grid initially unknown. The proposed method mainly consists of two parts that control design of grid connected inverter based on the PR controller and estimator design for the grid voltage as well as phase angle. Initial stage, the proposed method not cause any damage to system due to the uncertainty in phase angle. To verify the proposed sensor-less voltage control of 2-KVA prototype grid connected inverter has constructed using the DSPTMS320F28335. Through the comparative simulation and experiments, it has been validated the proposed method work effectively and under uncertain grid such as imbalance and harmonic distortion.

REFERENCES

1. Adil Sarwar, M. S. J. Asghar, "Integrated maximum power point tracking and harmonic reduction in a grid interactive solar pv inverter," *journal of instrumentation technology & innovations*, vol 4, no 1, pp. 7-15, 2014.
2. A. Chatterjee., B. Mohanty, "Design and analysis of stationary frame PR current controller for performance improvement of grid tied PV inverter," in *Proceedings of IEEE 6th India International Conference on Power Electronics (IICPE), Gwalior (2014)*, pp. 1-6.
3. "Comparison study of phase-shifted full bridge ZVS converters", *IEEE 35th Power Electronics Specialists Conference, 2004, PESC 04, volume 1*, pp: 533 - 539. 20-25 June 2004.
4. "High-frequency link inverter for fuel cells based on multiple-carrier PWM", *IEEE Transactions on Power Electronics volume 19, issue 4, Sept. 2004* pp: 1279 - 1288.
5. Krismadinata, N. A. Rahim and J. Selvaraj, "Implementation of hysteresis current control for single-phase grid connected inverter," in *Proceedings of the International Conference on Power Electronics and Drive Systems, Bangkok, Thailand (2007)*, pp. 1097-1101
6. M. Calais, J. Myrzik, T. Spooner, and V. Agelidis, "Inverters for single phase grid connected photovoltaic systems—an overview," in *Proc. IEEE Power Electron. Spec. Conf., Jun. 2002*, pp. 1995-2000.